Octobre 1987 LRP 327/87

TURBULENT DENSITY FLUCUTATIONS IN THE TCA TOKAMAK

H. Weisen, Ch. Hollenstein, R. Behn

To be published in Plasma Physics and Controlled Fusion

TURBULENT DENSITY FLUCTUATIONS IN THE TCA TOKAMAK

H. Weisen, Ch. Hollenstein, R. Behn

Centre de Recherches en Physique des Plasmas
Association Euratom - Confédération Suisse
Ecole Polytechnique Fédérale de Lausanne
21, Av. des Bains, CH-1007 Lausanne, Switzerland

ABSTRACT

The results of our investigation on the spectral characteristics, spatial structure and scaling with plasma parameters of low frequency density fluctuations in ohmically heated TCA plasmas are presented. A substantial fraction of the spectral energy is found to be associated with fairly small perpendicular wave numbers, $\langle k_\perp \rangle \lesssim 2$ rad/cm. Profile measurements indicate that the edge is dominated by low frequencies ($\lesssim$ 100 kHz) whereas the higher frequencies ($\gtrsim$ 100 kHz) dominate in the interior. An asymmetry between the low and the high field side is observed, confirming observations on two different machines. The estimated local level of the fluctuations and its scaling with plasma parameters is found to follow Kadomtsev's mixing length rule $\tilde{n}/n \cong (\langle k_\perp \rangle L_n)^{-1}$.

I. INTRODUCTION

Low frequency broadband turbulent fluctuations have been studied extensively over more than a decade in fusion research devices, using electromagnetic wave scattering techniques (MAZZUCATO, 1976; HAMBERGER et al., 1975; KOECHLIN et al., 1977; EQUIPE TFR 1983; CROWLEY and MAZZUCATO ,1983; SLUSHER and SURKO, 1980; TFR GROUP and TRUC, 1984 & 1986; Van ANDEL et al., 1987; BROWER et al., 1985a) and b)) the bulk of these observations, together with measurements using Langmuir probes in the edge plasma (ZWEBEN and GOULD, 1981; ZWEBEN, 1985; RITZ et al., 1984; SCHMITZ et al., 1985; LEVINSON et al., 1984) show that the fluctuations exhibit many features of drift wave turbulence. Nonetheless our knowledge remains uncomplete on several important issues. They concern the turbulence spectra at small wave numbers, the position dependence of the fluctuation amplitude, the relation between turbulence and anomalous transport, and even its basic nature (electrostatic or electromagnetic?). Among these four points only the former two can be investigated, at least partly, by optical diagnostics. With scattering diagnostics the main difficulty is due to the fact that there is always a trade-off between spatial resolution and wavenumber resolution. This difficulty, often in conjunction with access restrictions, seems to have led most investigators to adopt fairly small probe beam widths of typically one centimetre, thereby precluding reliable studies in the wavelength range above about one to two centimetres. At longer scale-lengths the wavenumber spectrum remains unresolved, and for some detection schemes there also is a sensitivity drop at wavenumbers below the resolution limit (see e.g. WEISEN, 1986b)). As a result the region $k_\perp \sim \rho_s^{-1}$ corresponding to the most unstable electrostatic drift waves, has

received a good deal of attention, whereas the small wavenumber region $k_\perp << \rho_s^{-1}$, is still poorly explored. ($\rho_s = c_s/\omega_{ci}$ is the ion Larmor radius with electron temperature).

The small wavenumber region may however contribute substantially to the fluctuation power as shown by the above referenced probe measurements (where $<k_\perp>\rho_s \sim 0.1$) and by correlation measurements using the phase contrast method (WEISEN et al., 1986). From a theoretical point of view, fluctuations with $k_\theta \rho_s << 1$ may arise by inverse cascading of spectral energy from the most unstable domain of electrostatic drift waves (HASEGAWA, MIMA, 1978), or they may be due to different unstable modes, like microtearing (DRAKE, LEE, 1977; CHEN et al., 1977) or rippling modes (ROGISTER, 1986).

II. EXPERIMENT

The measurements presented here were obtained in ohmically heated TCA plasmas (B_T = 15 kG, R = 61 cm, a = 18 cm, $I_p \leqslant 170$ kA, $\bar{n} \leqslant 10^{14} cm^{-3}$) using the phase contrast method. This imaging method avoids the above mentioned difficulties of scattering methods at long wavelengths (WEISEN, 1985 & 1986). It is suitable for the investigation of fluctuations in a wide band of wavenumbers, $0.5 \leqslant k_\perp \leqslant 20$ rad/cm for the measurements presented here. The experimental setup is described elsewhere (WEISEN 1986a). A 23 x 4cm wide CO_2 laser beam (λ = 10.6μ) is transmitted through the plasma via two NaCl windows. The optical system produces an image of the plasma where the small phase shifts ($|\phi| \sim 10^{-3}$radians) due to refractive perturbations are revealed as

corresponding intensity variations and are detected by liquid nitrogen cooled HgCdTe detectors. In the wavenumber range indicated the device is equivalent to a fast high resolution (1-2 mm) imaging interferometer with high sensitivity (10^{-5} radians for Δf = 1MHz).

Figure 1 shows a schematic of the optical arrangement and the fraction of the plasma cross section that is accessible. The two available detectors, D_1 and D_2 in Fig. 1, can be positioned independently in the image Σ' of the plasma midplane Σ. At CO_2 wavelengths the depth of field exceeds by far the dimensions of the plasma. Therefore the measurements are line integrated and free of scintillation effects which occur for out-of-focus imaging.

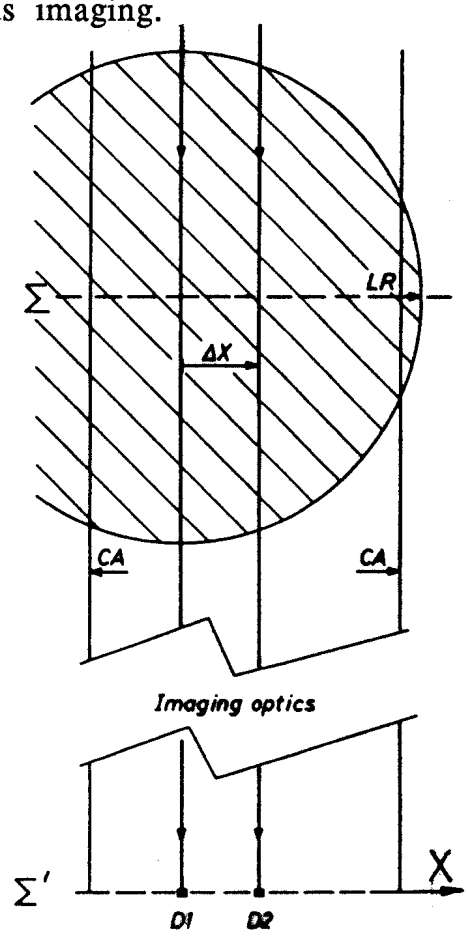

Fig. 1- Schematic of optical arrangement.
Σ : object plane at plasma midplane,
Σ' : image plane with detectors D_1 and D_2,
CA : Clear aperture of 23 cm,
LR : outer limiter radius,
x : position coordinate in Σ and Σ' (center : x = 0).

For correlation measurements, the data were acquired by synchronized Le Croy TR8837F transient digitizers (8 bit resolution, 8k samples). For monitoring the time evolution of the mean amplitude measured by a single detector, a bank of 8 half-octave filters ($\Delta f/fo$ = 0.31) covering the range 40 - 670 kHz was used.

Unless otherwise specified the results were obtained under stationnary conditions with an electron line density $\bar{n} = 2.5 \cdot 10^{13} cm^{-3}$, a safety factor at the limiter radius, $q(a) \cong 3.3$, a toroidal field B_T of 15 kG and a central electron temperature $T_e(0) \cong 800eV$.

III. SPECTRAL CHARACTERISTICS

The frequency spectra of the density fluctuations observed depend on the position x of the viewing chord (Fig. 2). For positions close to the plasma center ($x/a \lesssim 1/2$) the spectra are higher in frequency than those obtained for chords close to the edge. The latter are very similar to the ion saturation current spectra obtained from Langmuir probes in the scrape-off layer (HOLLENSTEIN et al. 1986).

Information on the spatial structure is obtained by correlation measurements using the two detectors. During these measurements detector D_1 was fixed whilst detector D_2 was scanned on a shot-to-shot basis in the vicinity of D_1. The cross-spectrum

$$P_{12}(f) = \langle I_1^*(f)\, I_2(f) \rangle$$

was obtained by averaging $I_1^*(f)I_2(f)$ over the 32 segments into which

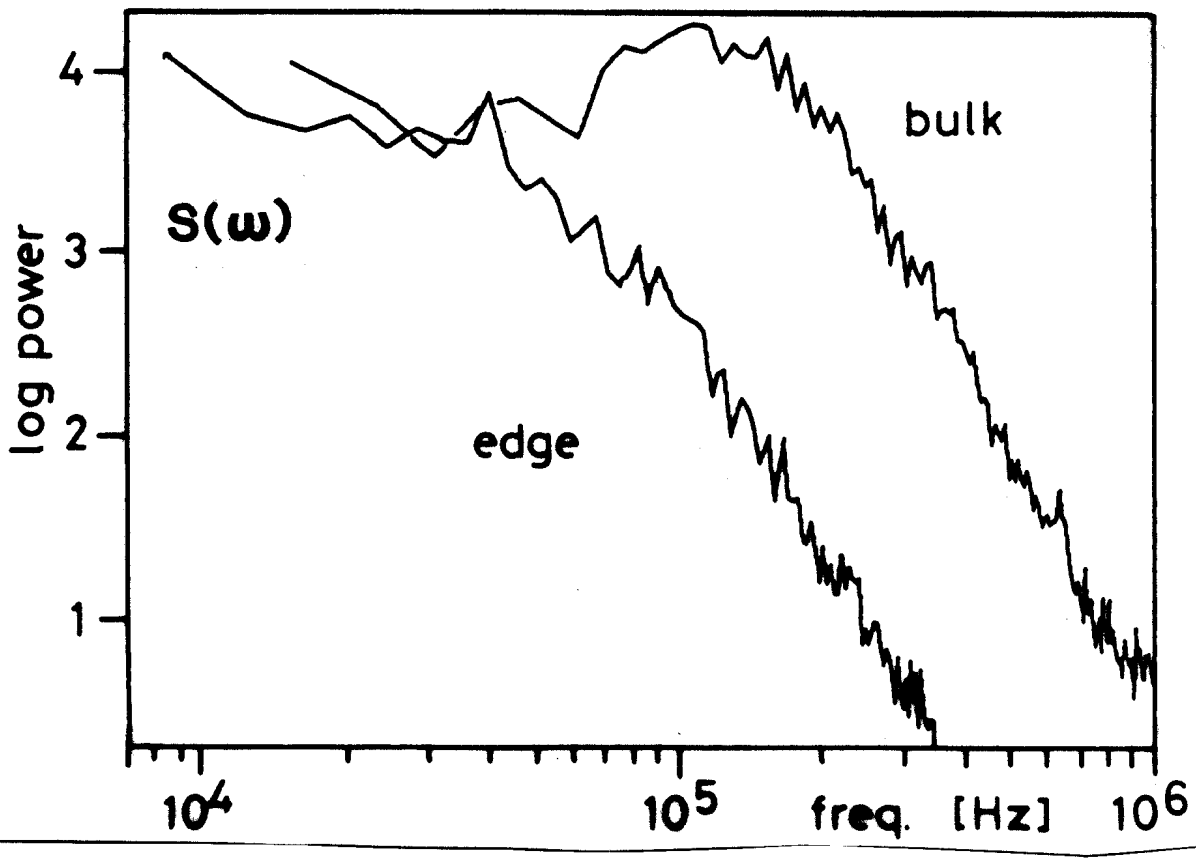

Fig. 2- Frequency spectra of low frequency turbulence for chords passing through the plasma centre and through the edge, at 1cm from the outer limiter.

the total record length of 8192 samples was divided. $I_1(f)$ and $I_2(f)$ are the Fast Fourier Transforms of the respective detector signals.

Figure 3 shows the real part of the normalized cross power $\gamma(\Delta x,f) \equiv \gamma_{12}(f) \equiv P_{12}(f)\{P_{11}(f)P_{22}(f)\}^{-1/2}$ as a function of chord separation $\Delta x = x_2-x_1$. Detector D_1 viewed a chord passing through the centre ($x_1 = 0$). For this geometry, the measurements reflect the poloidal autocorrelation function of the density fluctuations. The imaginary part of γ was consistently one order of magnitude smaller than the real part for these measurements. The absence of the imaginary part is easily explained if one assumes that the probe beam encounters approximately equal amounts of uncorrelated, spectrally equivalent perturbations propagating in opposite directions. (The two opposite directions along the x-axis are believed to correspond to the top and

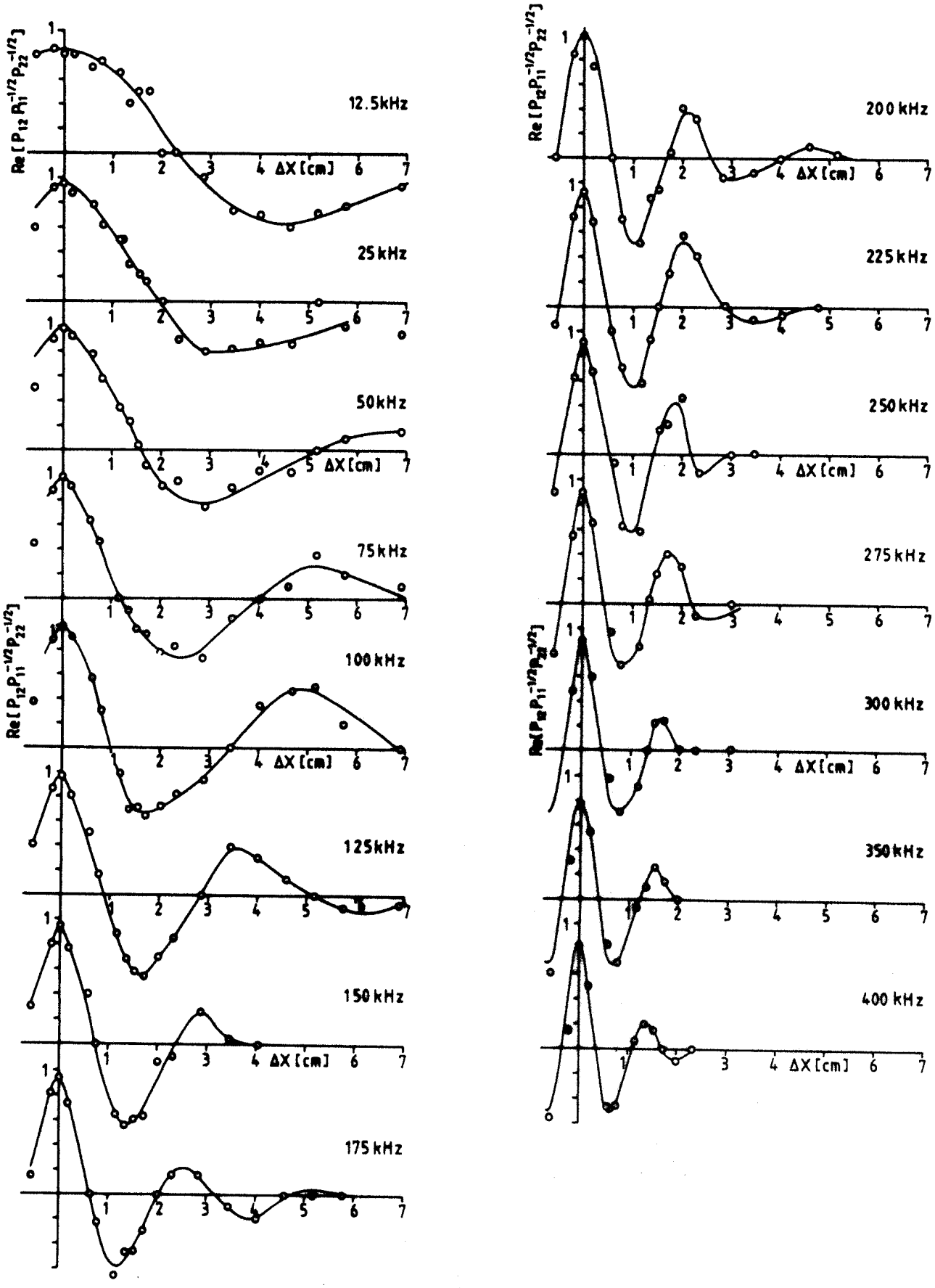

Fig. 3- Real part of normalized cross-correlation functions $P_{12}(\Delta x, f)$ of the line integrated density fluctuations. Detector D_1 viewed a chord through the centre while the position of detector D_2 was scanned from shot to shot.

bottom crossings of the viewing chords by fluctuations propagating poloidally in the electron drift direction, as reported from most heterodyne scattering experiments. We should note that in some other instances evidence for unidirectional propagation has also been found which may be indicative of top-bottom asymmetries (see BROWER et al. 1985a).)

In principle, if the turbulence is homogeneous, and if time averages are equivalent to spatial averages, the wavenumber spectrum can be obtained from these correlation measurements (in a non homogeneous plasma the wavenumber spectrum is ill defined). The spatial Fourier transform of $\gamma(\Delta x,f)$ yields a conditional spectrum $s(k|f)$, and subsequent multiplication by the frequency spectrum $s(f) \propto P_{11}(f)$ provides the complete spectrum $s(k,f)$ shown on Fig. 4 ($k \cong k_\theta$). Summing over frequencies yields the wavenumber spectrum $s(k)$ of Fig. 5. Both $s(k)$ and $s(k,f)$ have a maximum at $k = 1.3$ rad/cm, corresponding to $k\rho_s \cong 0.25$ if a typical electron temperature of 400 eV is assumed. Both $\gamma(\Delta x,f)$ and $s(k,f)$ show a clear dispersion with an average phase velocity of $5 \cdot 10^5$ cm/s. The conditional wavenumber spectra $s(k|f)$ are surprisingly narrow in spite of the line averaged character of the measurement, $\Delta k/k_{max} = 0.5$ to 0.7 at FWHM. Given the observed dispersion, the decrease of $s(k)$ at large k is expected to follow the same power law as $s(f)$, i.e. $s(k)$, $s(f) \propto k^{-\alpha}$, with $\alpha = 3.5 \pm 0.5$ (HOLLENSTEIN et al., 1986).

Unfortunately, due both to fact that the turbulence is not uniform as a function of position (see section III) and because of experimental errors, the Fourier transforms of the experimental correlation functions $\gamma(\Delta x,f)$ are not guaranteed to be positive. The resulting errors being about 10% of the maximum value of $s(k|f)$, the contour lines of Fig. 4 are

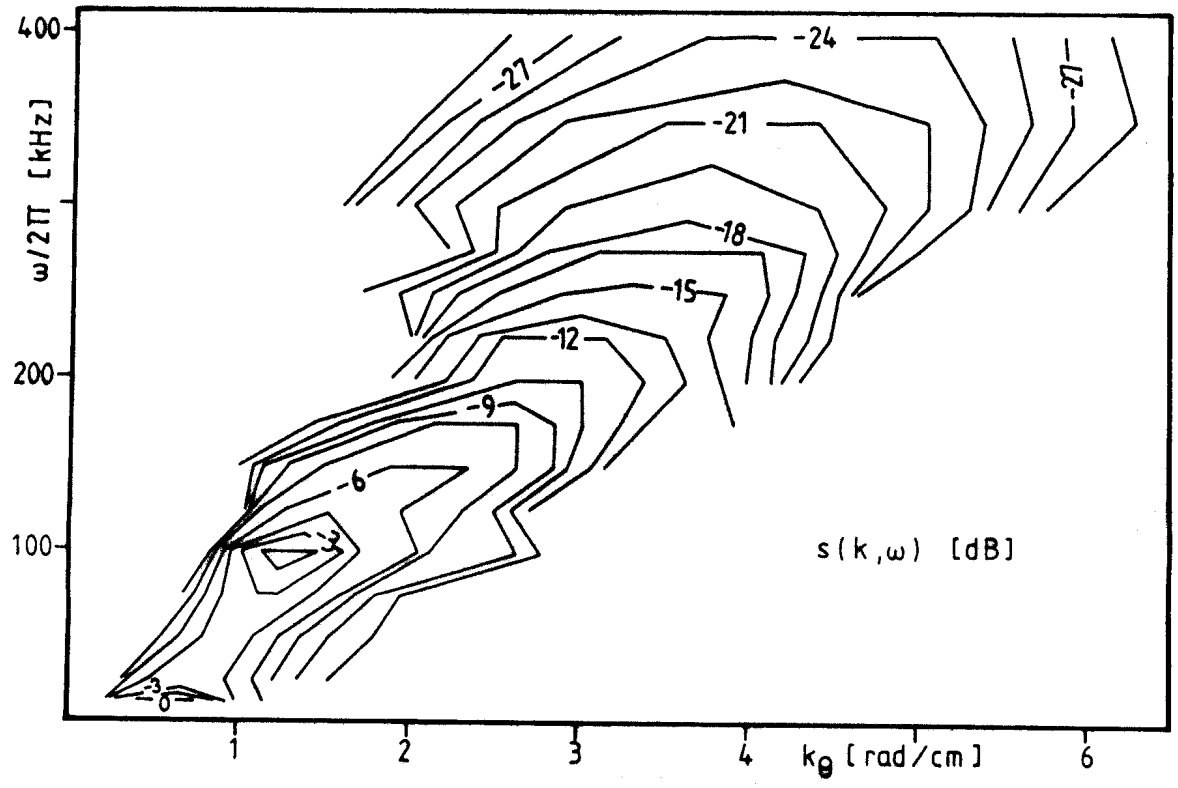

Fig. 4- Power density spectrum s(k,f) obtained from a Fourier transform on the data of Fig. 3 ($\underline{k} \equiv (k_\theta,0)$). The spacing of contour lines is a factor of 1.4.

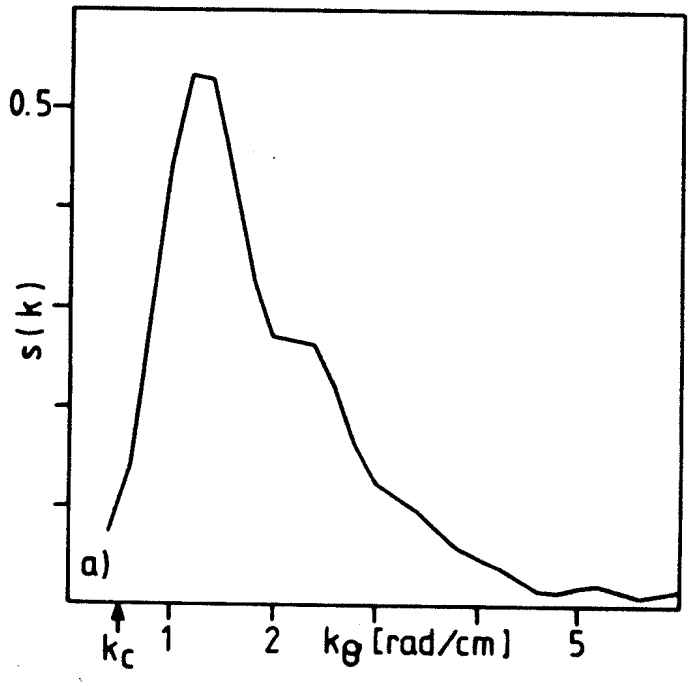

Fig. 5- Wavenumber spectrum corresponding to Fig. 4. (For T_e = 400 eV, k_θ = 1 rad/cm corresponds to $k_\theta \rho_s$ = 0.2).

only given for $s(k|f) > 0.1 \cdot s(k_{max}|f)$.

These measurements were repeated with the position of the reference chord viewed by detector D_1 at $x_1/a = 1/2$ and 3/4. The correlation functions $\gamma(\Delta x,f)$ remain similar in shape, as shown on Fig. 6a for f=100 kHz, but the wavelengths (at fixed frequency) diminish by a factor of 2 as the plasma edge is approached (see also WEISEN et al., 1986). The results for $x_1/a=1/2$ obtained for $\bar{n} = 2.5 \cdot 10^{13} cm^{-3}$ and for $\bar{n} = 5 \cdot 10^{13} cm^{-3}$ do not indicate a significant dependence of $\gamma(\Delta x,f)$ on the plasma density. Whereas the measurements near the edge are essentially radial correlations, the ones for $x_1/a = 1/2$ have a mixed (radial and poloidal) character.

Wavenumber spectra have not been computed from these correlation measurements because of the lack of homogeneity near the edge. The dominant scale lengths near the edge are however the same than for the interior because both the dominant frequencies and the widths of the correlation functions (at fixed frequency) are reduced by the same factor of 2-3. Remarkably, the dominant scales are also similar in the scrape-off layer. This can be infered from the wavenumber spectrum of Fig. 7 evaluated from the ion saturation current fluctuations of a pair of poloidally separated Langmuir probes according to a method introduced by BEALL et al. (1982).

A dispersion relation can be obtained directly from the correlation measurements if we define a mean wavelength Λ_{typ} as on Fig. 6a. Fig. 6b shows the frequency as a function of $k_{typ} = 2\pi/\Lambda_{typ}$. (The dispersion curves of Fig. 6b do not represent local dispersion relations but weighted averages over the plasma cross section). For the

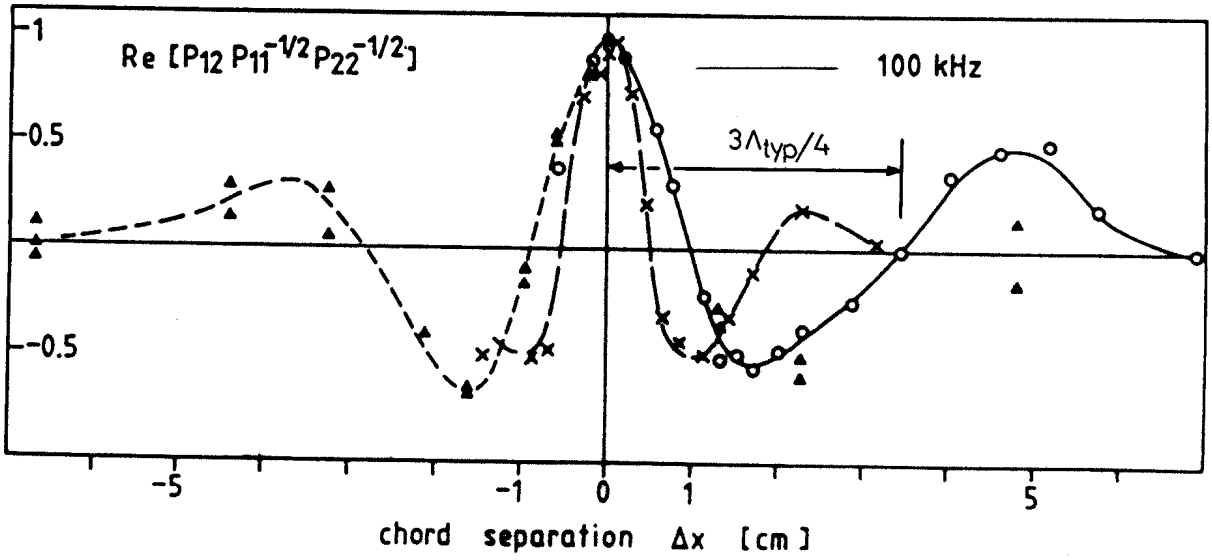

o: $x_1/a = 0$, $\bar{n}_{e13} = 2.5$; Δ: $x_1/a = 1/2$, $\bar{n}_{e13} = 2.5$; ▲: $x_1/a = 1/2$, $\bar{n}_{e13} = 5$; ×: $x_1/a = 3/4$, $\bar{n}_{e13} = 2.5$

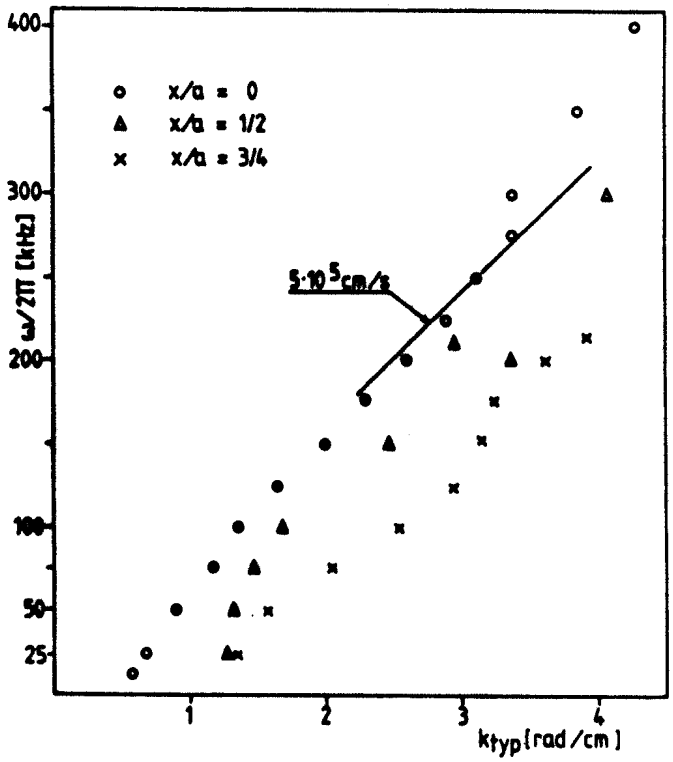

Fig. 6- a) As Fig. 3 for f=100 kHz but for various positions of detector D_1 :
circles : $x_1 = 0$ (centre),
crosses : $x_1/a = 3/4$ (edge),
triangles : $x_1/a = 1/2$ (mid-radius, full triangles correspond to $\bar{n} = 5 \cdot 10^{13}$ cm^{-3}).
b) frequency as a function of mean wavenumber $k_{typ} = 2\pi/\Lambda_{typ}$ from the above correlation measurements.

wavenumber range containing most of the spectral power, $1 < k_{typ} < 2.5$ rad/cm, the average transverse velocity $v_x = f \cdot \Lambda_{typ}$ decreases from about $5 \cdot 10^5$ cm/s in the central region to less than half this value near the edge. This observation was confirmed in an experiment where the two detectors were scanned accross the available aperture while maintaining a fixed separation of $\Delta x = 1.6$ cm. Inspection of the phase of the cross spectra $P_{12}(f)$ provided a velocity profile for the dominant part of the spectra ($k_\perp \sim 2$ rad/cm, Fig. 8). The plasma parameters in this experiment were $\bar{n} = 2.9 \cdot 10^{13} cm^{-3}$, R = 63 cm, a = 16 cm, q(a) = 3.3. (Unlike in the previous experiments the imaginary part of $P_{12}(f)P_{11}^{-1/2}P_{22}^{-1/2}$ was of the same order than the real part).

There are two possible interpretations of the differences in scale length and phase velocity v_x observed for chords passing through the interior and edge chords. They may be attributed to an anisotropy of a factor of two between the poloidal and the radial directions as suggested earlier (WEISEN et al., 1986), or, if the fluctuations are isotropic, show a decrease of the poloidal velocity from about $5 \cdot 10^5$ cm/s in the interior to about $2 \cdot 10^5$ cm/s near the edge. The explanation based on an anisotropy is only satisfactory if most of the observed turbulence originates from the edge as it is the case for low frequencies. This is not the case for the higher frequencies (f > 100kHz), as will be shown in section IV. The interpretation of a lower poloidal velocity near the edge is reinforced by correlation measurements using an array of visible light diodes mounted in the back of a camera and viewing over half of a plasma cross section the D_α emission from the edge along 15 nearly vertical chords with a spacing of 1.6 cm. The velocities v_x obtained were in the range 10^5 - $2.5 \cdot 10^5$ cm/s for frequencies up to 30 kHz with no systematic dependence on the

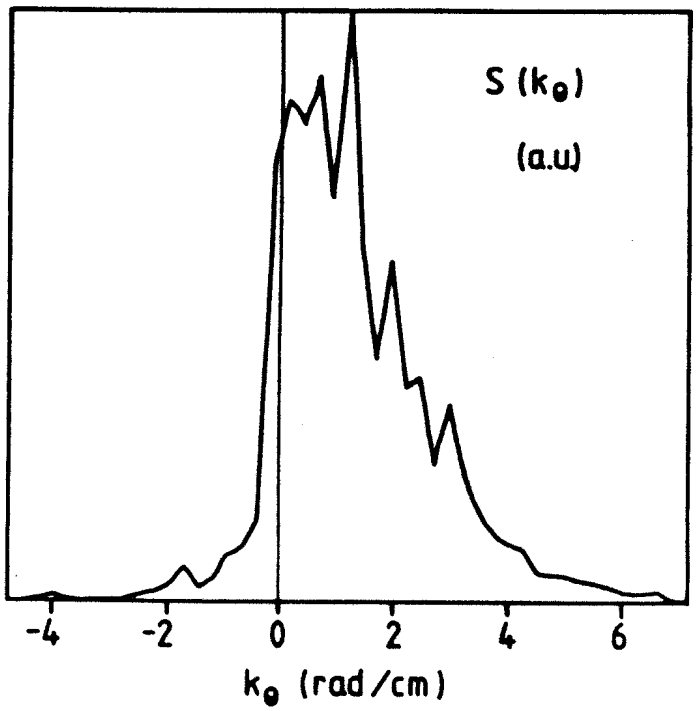

Fig. 7- Wavenumber spectrum $s(k_\theta)$ in the scrape-off layer of TCA obtained from a pair of Langmuir probes with a poloidal separation of 6mm. Propagation is predominantly in the ion diamagnetic direction.

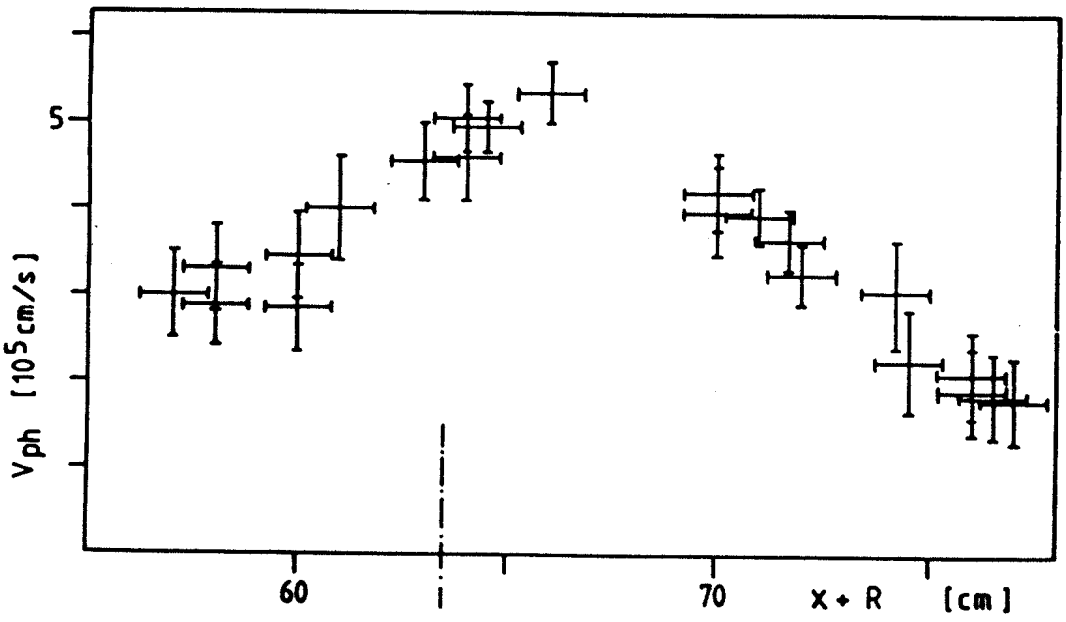

Fig. 8- Mean velocity of line integrated fluctuations obtained by scanning two detectors with a fixed separation Δx = 1.6cm. The ends of the horizontal bars indicate the detector positions. The plasma center is indicated by the vertical dotted line. (The in-out asymetry of v_x is believed to be a consequence of the in-out asymetry of the fluctuation amplitude, see Fig. 9.)

positions of the viewing chords (WEISEN, 1986a). (The observable frequency range for flucutations of D_α emission is limited to about 30kHz by ionization and recombination rates.)

The poloidal velocities (ion diamagnetic direction) obtained from Langmuir probe measurements in the scrape-off layer are widely variable as a function of distance to the limiter radius and range from 10^5 to 10^6 cm/s (HOLLENSTEIN et al., 1987).

IV. SPATIAL DISTRIBUTION AND AMPLITUDE

The spatial profiles of line integrated rms fluctuation levels obtained in a series of reproducible shots are shown in Fig. 9 for six of the channels of the half octave filter bank. The continuous lines correspond to a line density of $2.5 \cdot 10^{13}$ cm^{-3}, the broken ones to $\bar{n} = 4.5 \cdot 10^{13}$ cm^{-3}. The levels are expressed in milliradians of rms phase shift of the probe beam and are normalized to a line density of $2.9 \cdot 10^{13}$ cm^{-3}. We see that for $f \lesssim 100$ kHz the amplitude profile is peaked near the edge, whereas for $f \gtrsim 140$ kHz it peaks in the plasma interior at $x/a \cong 1/3$ on the low field side. The fluctuation amplitude on the low field side at $x/a = 0.25$ is about twice the amplitude at $x/a = -0.25$, indicating the importance of toroidal effects. Similar asymmetries had already been observed on the TEXT and PDX tokamaks (BROWER et al., 1985a, CROWLEY, MAZZUCATO 1985).

An inversion of the profiles of Fig. 9 is possible in principle (see appendix), but would require ad-hoc assumptions on both the spatial symmetry and the isotropy of the fluctuations, which would be difficult to justify. We thus do not believe an inversion to be reliable enough to

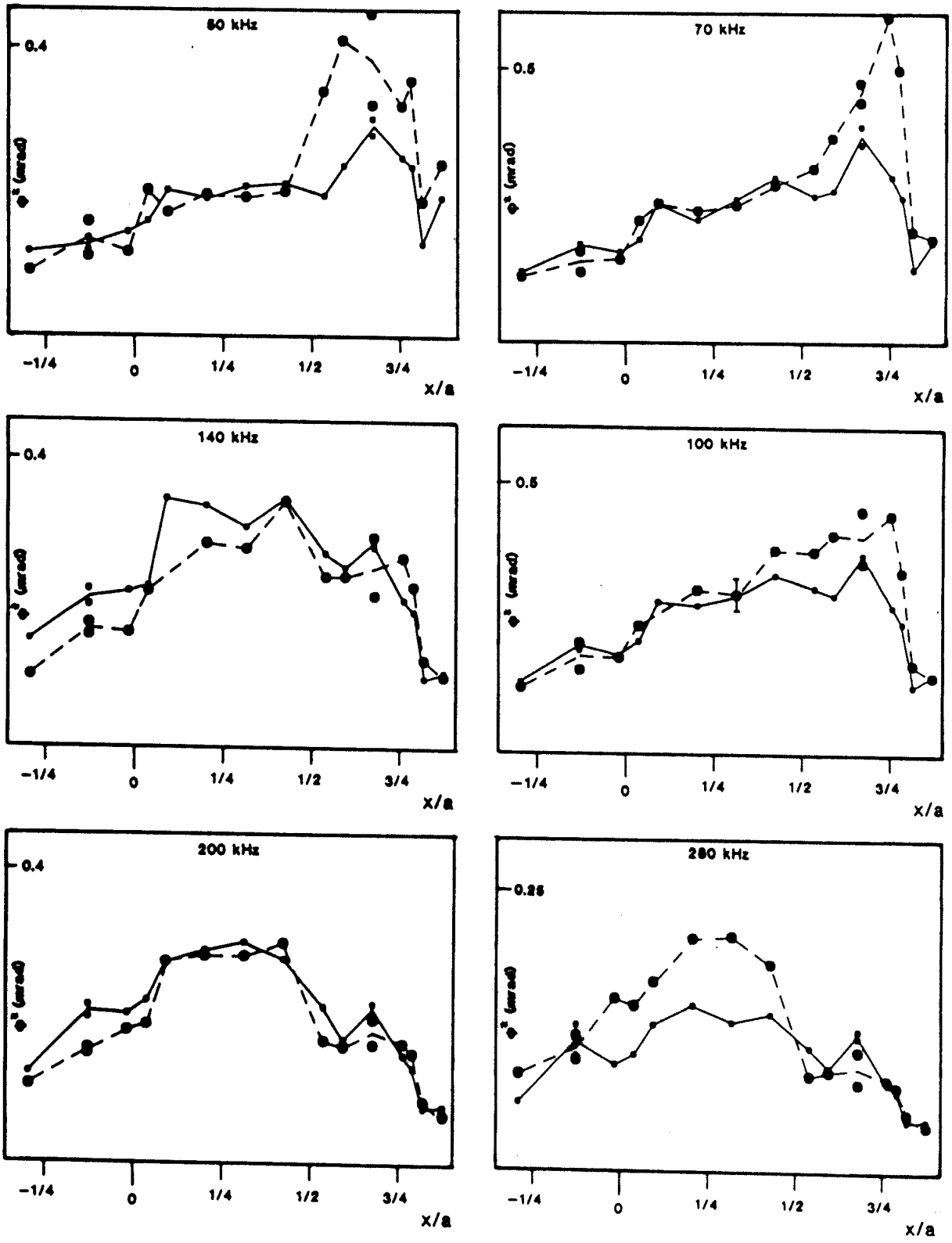

Fig. 9- Fluctuation amplitude profiles
Small symbols : $\bar{n} = 2.5 \cdot 10^{13}$ cm^{-3},
Large symbols : $\bar{n} = 4.5 \cdot 10^{13}$ cm^{-3}.
Measurements obtained from a series of reproducible discharges using the half octave filter banc. The fluctuation amplitude is normalized to a line density of $2.9 \cdot 10^{13}$ cm^{-3} and is expressed as the rms phase shift ϕ of the probe beam.
$\phi^* = \phi\bar{n}/(2.9 \cdot 10^{13}$ cm$^{-3})$
(1mrad of phase shift corresponds to $3.55 \cdot 10^{12}$ electrons/cm^2)

provide accurate information about the radial profiles of the fluctuation levels. Qualitatively the raw data of Fig. 9, suggest that the radial $\tilde{n}_{rms}$ profiles peak near the edge around r/a = 3/4 for frequencies up to about 100 kHz, and further in the interior, around x/a = 1/2 for higher frequencies. The dispersion curves of Fig. 6b can now be interpreted in terms of chordal averages with weighting factors depending on the local amplitudes. Low frequencies ($f \lesssim 70$ kHz) are edge weighted and yield the smallest velocities, even in the case of central viewing chords. The highest frequencies ($f > 150$ kHz) which are dominated by the inner gradient regions ($r/a \lesssim 3/4$) yield velocities in excess of $3 \cdot 10^5$ cm/s for x/a=0, 1/2 and 3/4. Thus at high frequencies there is no evidence for a significant anisotropy, although at frequencies below about 140 kHz a moderate amount of anisotropy is possible.

The local fluctuation level (n_{rms}) can be estimated from the line integrated level $\tilde{N}_{rms}$ by the relation $\tilde{N}_{rms} = \tilde{n}_{rms} \cdot \sqrt{L \cdot l}$, where L is the extent of the turbulent region ($L \cong a$) and $l = l(f)$ is the correlation length (see appendix). Summing over the eight frequency channels of the filter bank, and using the respective correlation lengths for each frequency, as obtained from the correlation measurements presented in section II, we obtain relative fluctuation levels $\tilde{n}/n \cong 2.5\%$ for r/a = 1/2 (assuming L = a) and $\tilde{n}/n \cong 5$ to 7% for r/a = 3/4 (assuming L = 12cm. Given the observed inhomogeneity and a possible moderate amount of anisotropy, L,l and thus the local fluctuation level can only be estimated within a factor of two). The relative fluctuation level thus appears to increase towards the plasma edge. In the scrape-off layer the amplitude measured by the ion saturation current of Langmuir probes reaches values of 20 - 40% rms. These values are close to Kadomtsev's mixing length level (KADOMTSEV, 1965), $\tilde{n}/n \cong (\langle k_\perp \rangle L_n)^{-1}$,

as $\langle k_\perp \rangle \cong 2$rad/cm throughout the plasma and $L_n \cong 18$, 7 and 2 cm for x/a = 1/2, 3/4 and 1.1 respectively.

Figure 10a) shows the line integrated rms fluctuation level as a function of line density for the entire bandwidth covered by the filter banc (40 - 670 kHz) for a central chord. We see that the scaling of N_{rms} with density also follows the mixing length rule $\tilde{N}_{rms}/\bar{n}$ being roughly constant throughout the operational domain of TCA. The proportionality $\tilde{N}_{rms} \propto \bar{n}$ is well followed for frequencies up to about 200 kHz. As an example Fig. 10b) illustrates the case of f = 100 kHz which corresponds to the maximum of the spectral density. At frequencies above 200 kHz, in the tail of the frequency spectrum, the increase of $\tilde{N}_{rms}$ with density is stronger than linear and the scatter of the data is larger, as indicated in Fig. 10c) for the band 340 - 670 kHz. The high frequency behaviour

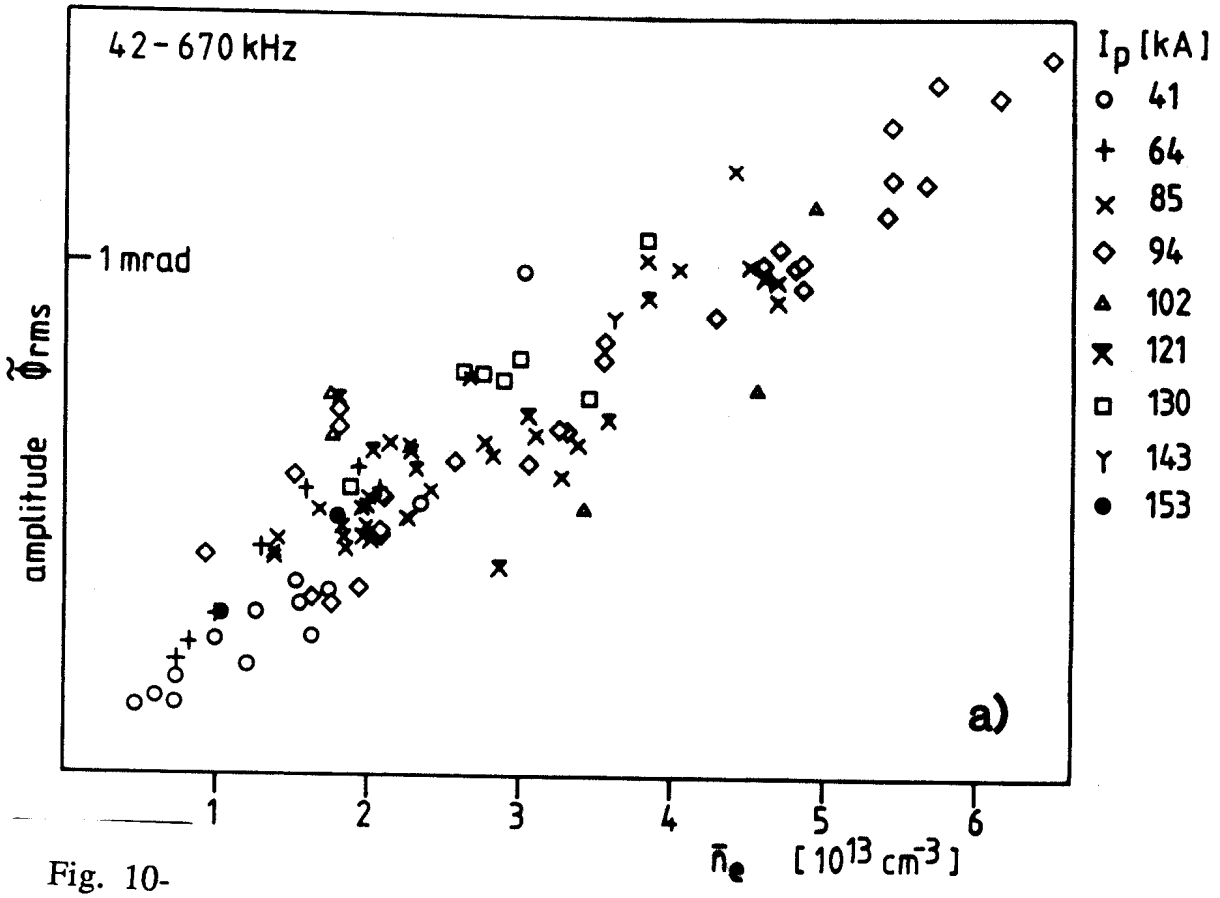

Fig. 10-

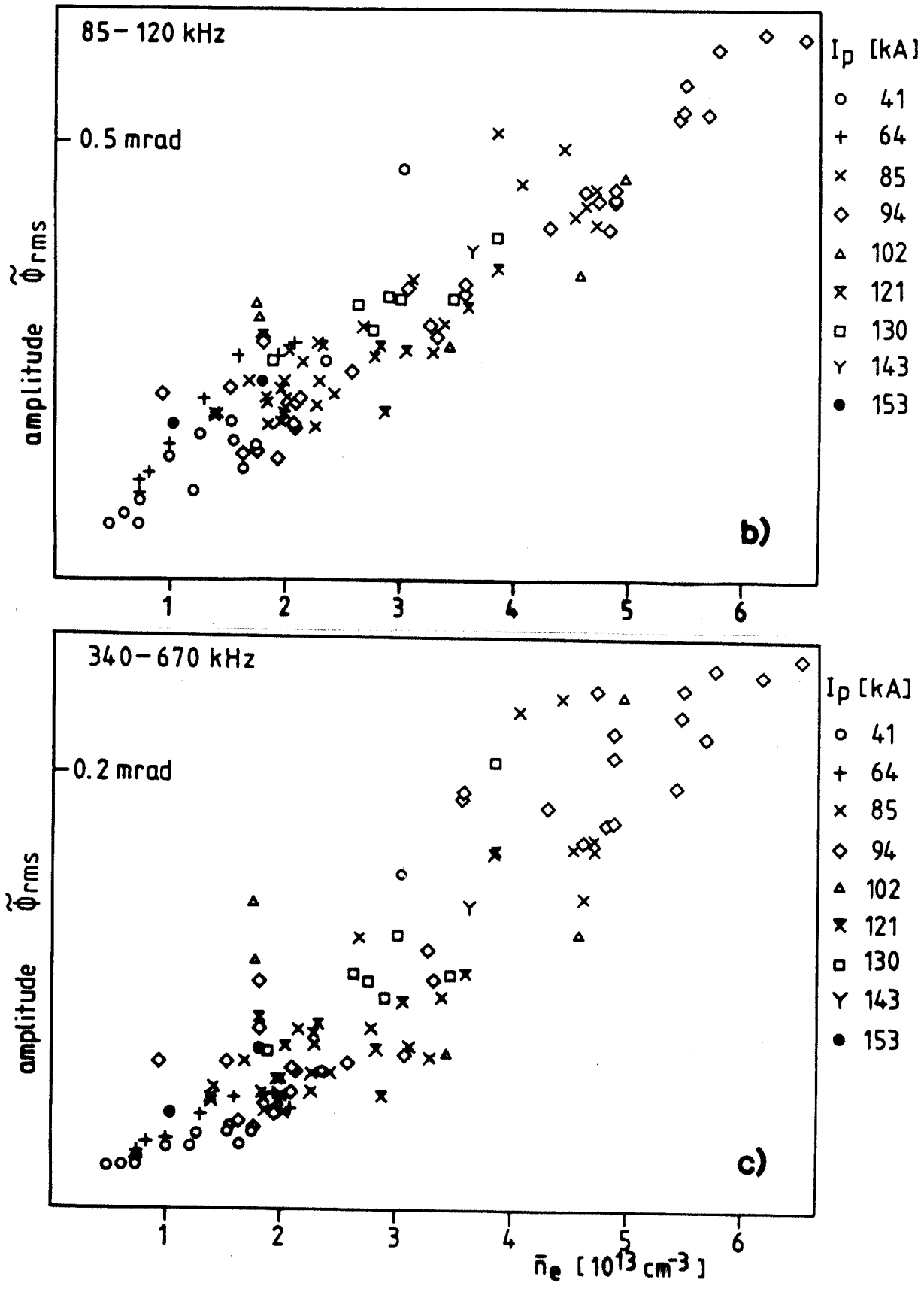

Fig. 10- Dependence of fluctuation amplitude on plasma parameters. Evaluated for a central chord for stationary conditions using the half octave filter banc.
a) rms amplitude for the entire frequency band covered by the filter banc,
b) rms amplitude for f_0 = 100kHz,
c) rms amplitude in the tail of the spectrum (f > 340kHz).

has little influence on the overall level, which is dominated by the frequency components below 200 kHz. This observation indicates that the turbulence level measured for a single frequency (or wavenumber) channel, particularly in the tail of the spectrum, can be a poor indicator of the overall fluctuation level.

We find no systematic dependence of the fluctuation level on the plasma current. In TCA the central electron temperature is proportional to the plasma current (JOYE et al., 1987). We would therefore expect a scaling $\tilde{N}_{rms} \propto \tilde{n}_{rms} \cdot \sqrt{lL}$ with $\tilde{n}_{rms} \propto \tilde{n}/(<k_\perp>L_n)$ from the mixing length rule. Neglecting changes in the profiles, and assuming that $l \propto <k_\perp>^{-1} \propto \rho_s \propto T_e^{1/2}$ the resulting scaling would be $\tilde{N}_{rms}/\bar{n} \propto T_e^{3/4} \propto I_p^{3/4}$ which is clearly not observed in the range of currents investigated (40 - 160 kA). The reason may be that $<k_\perp>$ does not depend on T_e as suggested by SURKO (1987). To clarify this point, correlation measurements for several plasma temperatures are needed.

V. DISCUSSION

Although the fluctuations observed appear to have the general features of drift wave turbulence, the possibility of an identification with any theoretical basic mode is very questionable. From the available experimental evidence it is not yet possible to decide whether to attribute them to the acoustic (essentially electrostatic) or Afvén drift wave branch.

The perpendicular velocities observed are about three times larger than the theoretical velocity for electrostatic drift waves

$v_D = cT_e \nabla n (enB_T)^{-1}$, but are in reasonable agreement with the diamagnetic drift velocity defined by $v_p = (\omega^* + \omega_T)/k_\theta = c\nabla p (enB_T)^{-1}$, as suggested by a comparison of Fig. 7 and 11. The latter shows the drift speeds v_p and v_D for modeled temperature and density profiles consistent with those observed on TCA. This observation confirms earlier results by BROWER et al. (1985a). The high velocity may suggest a relation with electromagnetic drift modes like tearing modes (DRAKE, LEE 1977; CHEN et al. 1977) or rippling modes (ROGISTER 1985). Incidentally, the observed poloidal velocity of $5 \cdot 10^5$ cm/s is very close to the poloidal velocity infered for the m = 2 MHD modes (Mirnov oscillations) in TCA (10 - 15 kHz, q = 2 at r ≅ 12 cm). The high velocities however can also be explained by superposed $\underline{E} \times \underline{B}$ fluid drifts if E_r derives from a potential $\Phi(r) = T_e(r)$ which could arise as a consequence of large electron losses.

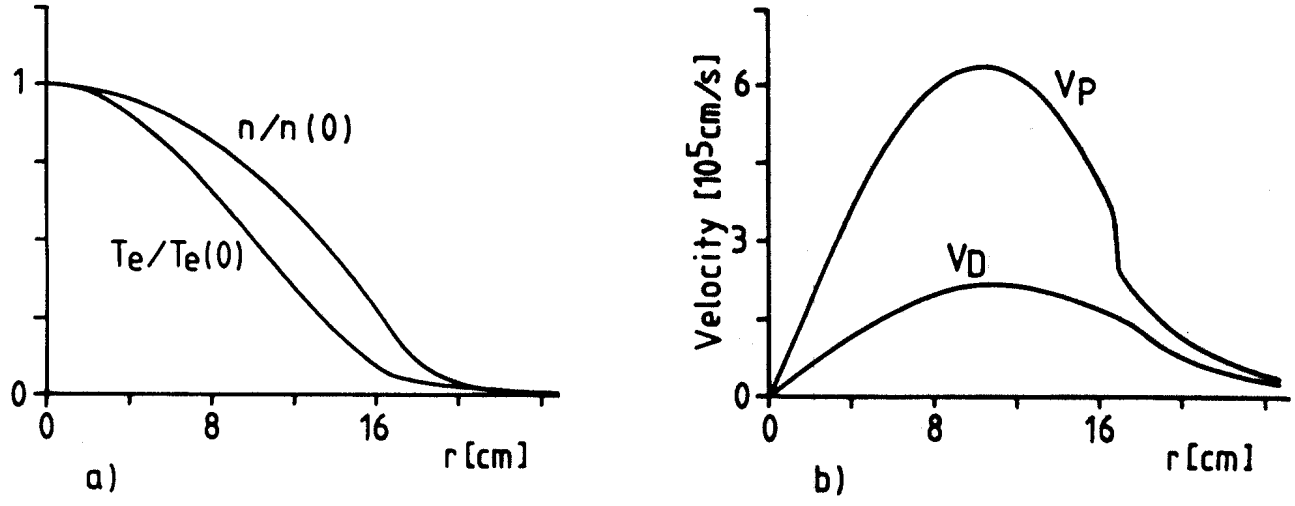

Fig. 11- Modeled electron temperature and density profiles (a) for TCA (parabolas to the power 2.5 and 1 respectively for r < 17cm) and resulting drift velocity profiles (b) for $T_e(0)$ = 800 eV.

The fairly low values of $k_\perp$ observed may result either from inverse cascading from the most unstable domain for electrostatic drift waves ($k_\theta \rho_s \sim 1$) or correspond to the most unstable electromagnetic modes. For TCA parameters the instability window of rippling modes (ROGISTER 1986), $0.1 \lesssim k_\theta \lesssim 1$ rad/cm, only falls slightly short of the maximum of s(k) of Fig. 5. On the other hand theoretical spectra for electrostatic trapped electron drift wave turbulence proposed by SEN and KIM (1986) are fairly similar to the spectrum of Fig. 5. Following their theory the decrease of s(k) for $k_\theta < 1$ rad/cm (corresponding to $k_\theta \rho_s < 0.2$) would have to be attributed to nonlinear shear damping, by which the energy cascade from the larger $k_\perp$ is terminated (TANGE et al. 1982). Experimentally this region needs further investigation due to the presence of an instrumental cutoff at $k_\perp = 0.5$ rad/cm.

It is fairly clear from the correlation measurements that the fluctuations do not strongly deviate from isotropy. This observation does not support electromagnetic drift modes, for which $k_r >> k_\theta$ according to current models, as a plausible cause of these fluctuations. Isotropy might however result from cascading. Also the observation of the Kinetic Alfvén Wave excited during Alfvén Wave Heating in TCA provides at least one example of an electromagnetic mode with radial wavenumbers (0.5 - 3 rad/cm) covering the range of those observed for turbulent fluctuations (BEHN et al., 1986).

In principle, if the wavenumbers parallel to the magnetic field could be measured, it would be possible to determine if the fluctuations belong to the drift Alfvén wave branch or to the acoustic drift wave branch. Ironically, the spatial modulation of the amplitude along field lines due to the in-out asymmetry suggest that the parallel

wavenumber spectrum contains components with $k_{||}=0$ and $k_{||}\approx 1/Rq$. Whereas the former belongs to the Alfvén drift branch, it is easily seen from the plasma parameters and the frequencies involved that the latter belongs to the acoustic drift wave branch. Thus the Alfvén and acoustic drift wave branches of slab geometry may well be coupled in a torus.

The small wavenumber capabilities of our instrument raise the question of whether there are any discrepancies with wavenumber spectra obtained from scattering diagnostics. In a recent letter SURKO (1987) compared the widths of the s(k) spectra reported from several experiments; the spectra were approximated by a Gaussian $s(k) \propto \exp(-k^2/\Delta k^2)$. His Fig. 1 suggests that Δk increases linearly with B_T, but is independent of the position of the measurement (edge or bulk). It turns out that the wavenumber for which s(k) has decreased to 1/e of its maximum value (Fig. 5), $k_\theta \approx 2.5$ rad/cm, is consistent with the spectral widths Δk reviewed on Surko's Fig. 1.

Assuming isotropic electrostatic turbulence the quasilinear heat flux $Q_t=5B\langle\tilde{p}\tilde{E}\rangle/2c$ can be estimated (KRALL, Mc BRIDE, 1977). Neglecting T_e fluctuations, and assuming $\tilde{E} \equiv \langle k_\perp\rangle\tilde{\Phi}$, with $\tilde{\Phi} = \tilde{n}T_e/n$, we obtain

$$Q_t = 4\cdot 10^{-4} \langle\tilde{n}^2/n^2\rangle\, nT_e^2 B_T^{-1} \langle k_\theta\rangle\, \gamma_{\tilde{E}\tilde{p}}$$

where $\gamma_{\tilde{E}\tilde{p}}$ describes the phase and coherence between $\tilde{p}$ and $\tilde{E}$ ($-1 < \mathrm{Re}\{\gamma_{\tilde{E}\tilde{p}}\} < 1$). The magnitude of the fluctuations is sufficient to produce heat fluxes of the order of the ohmic power in TCA. However, if Q_t really plays a dominant role, given the scaling observed ($\tilde{n}/\bar{n} \equiv$ cst), one has to assume that $\gamma_{\tilde{E}\tilde{p}}$ varies as a function of plasma parameters,

particularly that $\gamma\tilde{E}\tilde{p}$ scales like n^{-1}, as may arise from the trapped electron instability (KADOMTSEV, POGUTSE, 1971). (In TCA the inner two thirds of the plasma column are in the trapped electron regime i.e. $\nu^* = \nu_{ei}(\varepsilon\omega_{be})^{-1} < 1$ for the $r/a < 2/3$.) Unfortunately, due to their inability of measuring $\gamma\tilde{E}\tilde{p}$, the question of the relation between low frequency turbulence and confinement cannot be addressed with optical diagnostics alone.

VI. CONCLUSION

In this experiment we have used an imaging diagnostic based on the phase contrast method to investigate low frequency broadband turbulence in tokamak plasmas. By Fourier transformation of correlation measurements we obtain a wavenumber spectrum peaking around $k_\perp = 1.3$ rad/cm, which corresponds to $k_\perp \rho_s \cong 0.25$ in the plasma interior. Our profile measurements suggest that the fluctuations in the interior are of higher frequency and of higher velocity ($v_\theta \approx 5 \cdot 10^5$cm/s) than those observed near the edge ($v_\theta \approx 2 \cdot 10^5$cm/s) and in the scrape-off layer. The dispersion observed inside the limiter radius is consistent with the diamagnetic drift velocity $v_p = c\nabla p(enB_T)^{-1}$.

The estimated local level of fluctuation and its scaling with plasma density are in agreement with Kadomtsev's mixing length rule. At this level an induced heat flux of the order of the ohmic power is possible. The absence of a phase measurement between $\tilde{E}$ and $\tilde{n}$ however precludes any stronger statement on the role of the density fluctuations in plasma confinement.

Certainly more detailed observations than the ones presented here can still be expected from optical diagnostics. Nevertheless we believe that important progress will depend on diagnostics offering the possibility of also measuring fluctuations of plasma potential, magnetic field and temperature, and the phase relation between fluctuating quantities.

Acknowledgments

We would like to thank J.B. Lister, W.C. Simm, A. Pochelon, Liu Chen and Prof. F. Troyon for their support and stimulating discussions.

This work was partly supported by the Fonds National Suisse de la Recherche Scientifique.

REFERENCES

BEALL B.B., KIM Y.C. and POWERS E.J. (1982), J. Appl. Phys.53, 3933.

BEHN R., COLLINS G.A., LISTER J.B. and WEISEN H., (1987) Plasma Phys. & Contr. Fusion 29, 75.

BROWER D.L., PEEBLES W.A., LUHMANN N.C. and SAVAGE R.L. (1985a), Phys. Rev. Lett. 54,689.

BROWER D.L., PEEBLES W.A., LUHMANN N.C. and SAVAGE R.L. (1985b), Phys. Rev. Lett.55, 2579.

CHEN L., RUTHERFORD P.H. and TANG W.M. (1977), Phys. Rev. Lett. 39, 460.

CROWLEY T. and MAZZUCATO E., (1985) Nucl. Fusion 25, 507.

DRAKE J.F. and LEE Y.C. (1977) Phys. Fluids 20, 1341.

HAMBERGER S.M., SHARP L.E., LISTER J.B. and MROWKA S. (1976) Phys. Rev. Lett. 37, 1345.

HASEGAWA A. and MIMA K. (1978) Phys. Fluids 21, 87.

HOLLENSTEIN Ch., MARTIN Y., and SIMM W.C. (1987) J. Nucl. Mat. 145 - 147, 260.

HOLLENSTEIN Ch., KELLER R., POCHELON A., RYTER F., SAWLEY M.L., SIMM C.W. and WEISEN H., Int. Workshop on Small Scale Turbulence and Anomalous Transport in Magnetized Plasmas, Cargèse, July 1986 & CRPP report LRP 306/86.

JOYE B., LISTER J.B., MORET J.-M. and NOWAK S. (1987) Plasma Phys. & Contr. Fusion 29, 27.

KADOMTSEV B.B. (1965), "Plasma Turbulence" AP 1965.

KADOMTSEV B.B. and POGUTSE O.P. (1971), Nucl. Fusion 11, 67.

KOECHLIN F., CLAUDE V. and HOW J. (9177) Rev. Phys. Appl. 12, 1797.

KRALL N.A. and McBRIDE J.B. (1977) Nucl. Fusion 17 713.

LEVINSON S.J., BEALL J.M. POWERS E.J. and BENGSTON R.D. (1984) Nucl. Fusion 24, 527.

MAZZUCATO E. (1976) Phys. Rev. Lett. 36, 792.

RITZ Ch., ROGER D., BENGSTON S.J. LEVINSON S.J. and POWERS E.J. (1984) Phys. Fluids 27, 2956.

ROGISTER A. (1986), Plasma Phys. & Contr. Fusion 28, 547.

SCHMITZ L., LUETHEN S., DERRA G., BOEHM G., SCHLUETER H., (1985) Plasma Phys. & Contr. Fusion 27, 891.

SEN A.K. and KIM S.Y. (1986) Plasma Phys. & Contr. Fusion 28, 1009.

SLUSHER R.E. and SURKO C.M. (1980) Phys. Fluids 23, 472.

SURKO C.M. (1987), Comments on Plasma Phys. & Contr. Fusion 10, 265.

TANGE T., NISHIKAWA K. and SEN A.K. (1982), Phys. Fluids 25, 1592.

TFR Group (1983), Plasma Phys. 25, 641.

TFR Group and TRUC A. (1984), Plasma Phys. & Contr. Fusion 26, 1045.

TFR Group and TRUC A. (1987), Nucl. Fusion, to be published

VAN ANDEL H.W.H., BOILEAU A. and VON HELLERMANN M. (1987) Plasma Phys. & Contr. Fusion, 29, 49.

WEISEN H. (1985) Infrared Phys. 25, 543.

WEISEN H., SIMM C.W., POCHELON A., HOLLENSTEIN Ch. and BEHN R. (1986), Plasma Phys. & Contr. Fusion 28, 1161.

WEISEN H. (1986a), Thesis No 659 (1986), Ecole Polytechnique Fédérale de Lausanne, Chap. 6. (also CRPP report LRP 312/86).

WEISEN H. (1986b), Plasma Phys. & Contr. Fusion 28, 1147.

ZWEBEN S.J. and GOULD R.W. (1985) Nucl. Fusion 25, 171.

ZWEBEN S.J. (1985) Phys. Fluids 28, 974.

APPENDIX

Line integral in a random medium

The correlations that can be measured using an instrument without resolution along the line of sight, like an interferometer or our phase contrast device, are of the form

$$\bar{\Gamma}(x,t,\Delta x,\Delta t) = \langle \tilde{N}(x,t)\ \tilde{N}(x+\Delta x,t+\Delta t)\rangle\ , \tag{A.1}$$

where

$$\tilde{N}(x,t) = \int \tilde{n}(x,z,t)\ dz, \tag{A.2}$$

whereas the quantities of interest are the local correlations, which are of the form

$$\Gamma(x,z,t,\Delta x,\Delta z,\Delta t) = \langle \tilde{n}(x,z,t)\tilde{n}(x+\Delta x,z+\Delta z,t+\Delta t)\rangle\ . \tag{A.3}$$

The integral of (A.2) extends over the full region of interest, e.g. the turbulent plasma. (In this appendix we use a horizontal bar to distinguish chordal correlations from local correlations.) Using (A.2) and (A.3) in (A.1) we find

$$\bar{\Gamma}(x,t,\Delta x,\Delta t) = \iint \Gamma(x,z,t,\Delta x,\Delta z,\Delta t)\ d\Delta z dz\ . \tag{A.4}$$

The same relation exists between the temporal Fourier transforms of Γ and $\bar{\Gamma}$. In the case where the turbulent medium is homogeneous (Γ independent of x and z), then $\bar{\Gamma}$ is just a line integrated version of Γ, thus in the case of isotropy $\bar{\Gamma}$ is the Abel transform of Γ.

To estimate the variance of the line integral we introduce the correlation length

$$\ell_z(x,z,t) = \frac{\int \Gamma(x,z,t,0,\Delta z,0)d\Delta z}{\langle|\tilde{n}(x,z,t)|^2\rangle} \quad . \qquad (A.5)$$

and (A.4) becomes

$$\langle|\tilde{N}(x,t)|^2\rangle = \bar{\Gamma}(x,t,0,0) = \int \Gamma(x,z,t,0,0,0)\ \ell_z(x,z,t)dz \qquad (A.6)$$

If l_z is independent of z (e.g. homogeneous turbulence) we get for a length L of turbulent medium :

$$\langle|\tilde{N}(x,t)|^2\rangle \simeq \langle|\tilde{n}(x,z,t)|^2\rangle\ \ell_z L \ . \qquad (A.7)$$

A similar relation is obtained for the frequency spectra

$$\bar{S}(x,f) \simeq S(x,z,f)\ \ell_z(f)L$$

where

$$\ell_z(f) = \frac{\int\langle\tilde{n}^*(x,z,f)\tilde{n}(x,z+\Delta z,f)\rangle d\Delta z}{\langle|\tilde{n}(x,z,f)|^2\rangle} \quad . \qquad (A.8)$$

In each case we have an effective integration length $L_{eff}= \sqrt{l_z L}$. If the fluctuations are isotropic the correlation lengths can be calculated from the measured Γ. Fig. 12 shows one of the correlation functions of Fig. 3 and its Abel inversion calculated to estimate $l_z(f)$. Fig. 13 shows that for these correlation functions $l_z(f)$ is roughly equal to $\Lambda_{typ}/4$, Λ_{typ} being the "typical wavelength" at frequency f, as defined on Fig. 6. This value $l_z(f)=\Lambda_{typ}(f)/4$ was used to estimate the local fluctuation level in section IV.

The inverse problem is particularly difficult in a non homogeneous plasma. If the fluctuations are isotropic and have known spatial

symetries an Abel inversion of S(x,f) yields $S(r,f)l_z(r,f)$. Provided an independent estimate of $l_z(r,f)$ is available, the local variance can be obtained. If not, the inversions for the normalized correlation functions γ and for the local variance cannot be treated separately.

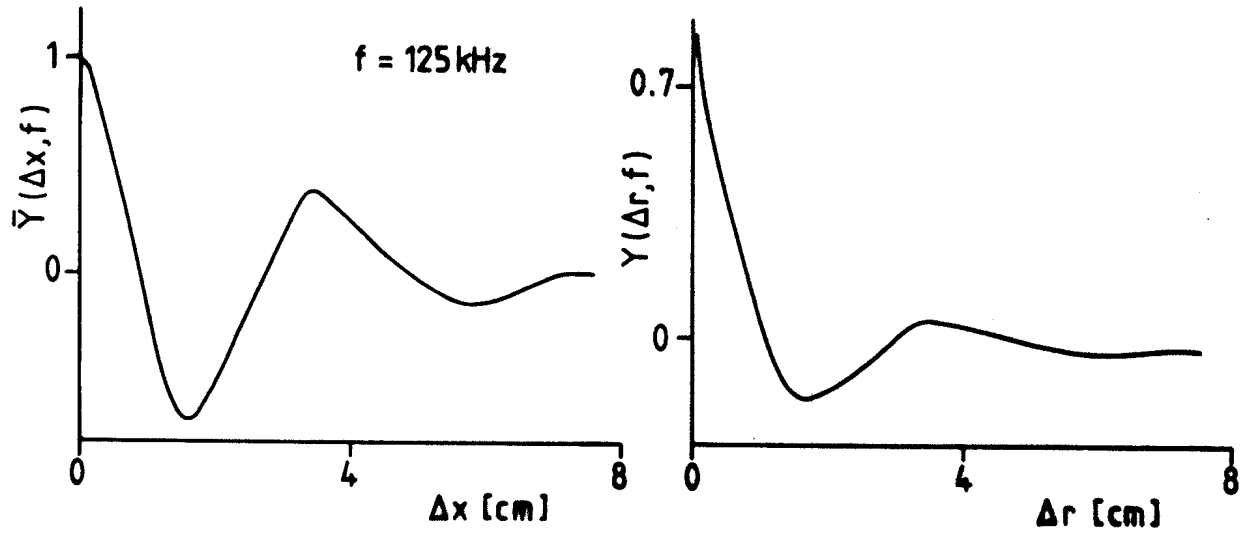

Fig. 12- Example of one of the correlation functions $\bar{\gamma}(\Delta x,f)$ of Fig. 3 and its inverse Abel transform $\gamma(\Delta r,f)$.

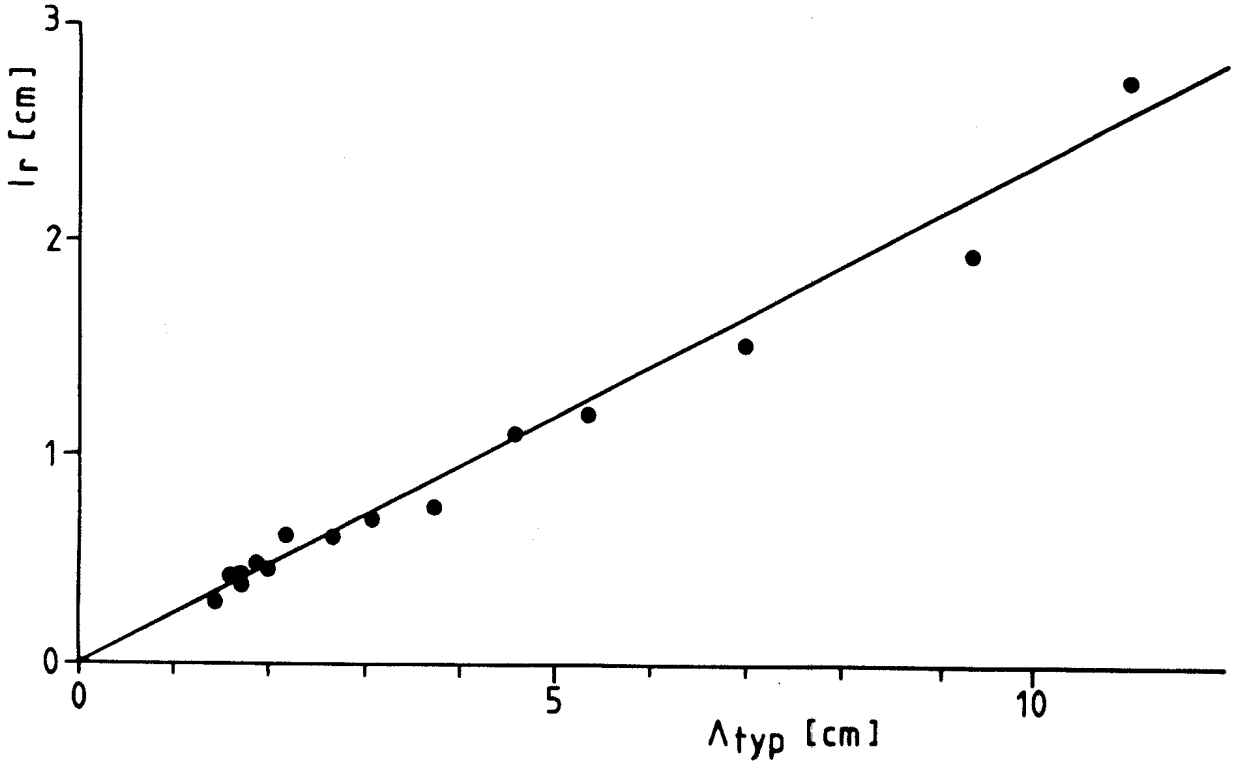

Fig. 13- Correlation length $l_r(f)$ obtained from $\gamma(\Delta r,f)$ as a function of $\Lambda_{typ}(f)$ defined on Fig. 6, showing that $l_r(f) \equiv \Lambda_{typ}(f)/4$.